Molecular Dynamics and Physical Stability of Amorphous Anti-Inflammatory Drug: Celecoxib

K. Grzybowska,* M. Paluch, A. Grzybowski, Z. Wojnarowska, L. Hawelek, and K. Kolodziejczyk

Institute of Physics, University of Silesia, ul. Uniwersytecka 4, 40-007 Katowice, Poland

K. L. Ngai

Naval Research Laboratory, Washington, D.C. 20375-53 USA

Received: May 3, 2010; Revised Manuscript Received: August 15, 2010

By using dielectric spectroscopy we analyzed the relation between molecular mobility and tendency of the amorphous celecoxib to recrystallize. We found that celecoxib is kinetically a fragile glassformer, contrary to the conclusion reached by others from thermodynamic fragility. The possible correlation of the large tendency of celecoxib to crystallize with various molecular motions have been investigated. Our study shows that the structural relaxation seems to be responsible for devitrification of celecoxib if stored at room temperature ~293 K. Notwithstanding, the crystallization can be considered to ultimately be affected by the β-process (JG-relaxation) because it is the precursor of the structural α-relaxation.

Introduction

Many crystalline drugs are poorly water-soluble, therefore they are limited in bioavailability. Preparation of the compounds in amorphous forms is a promising method for improving solubility of these drugs. It has been established that the solubility of amorphous pharmaceutical systems in water, such as amorphous celecoxib, is significantly higher than that of its crystalline counterpart.[1,2] Unfortunately, the amorphous state has higher energy than the crystalline state. Hence, usually it is not stable and may undergo recrystallization over the time course of processing, storage, and use of the product. Therefore, the main challenge in working with the amorphous form of drugs is the enhancement of their physical stability as well as proper identification and understanding of the physical factors that influence crystallization from the glassy state. Probably the most important factor determining stability of amorphous drugs is their molecular mobility.[3−5] For the purpose of determining molecular mobility, it is helpful to study the relaxation processes in the supercooled liquid and glassy states.

A useful method to determine time scales of molecular motions of pharmaceuticals in the glassy and liquid states is the broadband dielectric spectroscopy, which enables measurements of relaxation times over wide frequency range up to 12 decades, and at different temperatures and pressures. Glass-forming materials usually exhibit several relaxation processes of different nature in the dielectric relaxation spectra, which can be distinguished by their properties, including their dependence on temperature and pressure.

The dominant relaxation process in a supercooled liquid observed at temperatures T higher than the glass transition temperature T_g is a structural α-relaxation. It is a cooperative and correlated motion of many molecules together and it is responsible for the liquid-glass transition. The correlation function of the structural relaxation process, $\Phi(t)$, typically is a nonexponential function of time, and it can be described by the empirical Kohlraush−Williams−Watts (KWW) equation[6]

$$\Phi(t) = \exp\left[-\left(\frac{t}{\tau_\alpha}\right)^{\beta_{KWW}}\right],\ 0 < \beta_{KWW} \leq 1 \qquad (1)$$

where τ_α is the characteristic relaxation time, and the stretch exponent β_{KWW} is a fraction of unity. The complement, $n = 1 - \beta_{KWW}$, of the stretch exponent indicates the deviation from exponential (Debye) behavior. The parameter n correlates with the width of the frequency dispersion of the α-relaxation and can be considered as a measure of the degree of cooperativity, length scale, or dynamics heterogenity of the structural relaxation.[7,8]

During vitrification, the α-process enormously slows down. Such an extremely rapid increase in the structural relaxation times, τ_α, on isobaric cooling is the hall mark of the liquid-glass transition. An empirical Vogel−Fulcher−Tamman (VFT) equation,[9−12]

$$\tau_\alpha = \tau_\infty \exp\left(\frac{DT_0}{T - T_0}\right) \qquad (2)$$

is most commonly used to quantitatively describe the temperature dependence of α-relaxation times in the supercooled liquid up to the glass transition temperature T_g usually defined by $\tau_\alpha(T_g) = 100$s. In eq 2, τ_∞, T_0, and D are parameters determined by fitting the experimental data.

The dynamic "fragility" or "steepness index" m has been defined by Böhmer et al.[8] as follows

$$m \equiv \frac{\mathrm{d}\log\tau_\alpha}{\mathrm{d}\,(T_g/T)}_{T=T_g} = \frac{D(T_0/T_g)}{(1 - (T_0/T_g))^2 \ln(10)} \qquad (3)$$

* To whom correspondence should be addressed. E-mail address: kgrzybow@us.edu.pl.

10.1021/jp1040212
Published on Web 09/17/2010

Using the parameter m we can classify supercooled liquids into two types:[13] "strong" if the temperature dependence of τ_α is close to Arrhenius behavior in the plot of log τ_α vs scaled temperature T_g/T, and "fragile" if the temperature dependence of log τ_α deviates significantly from Arrhenius but it can be expressed by means of the VFT equation. The "strong" glassformers are usually characterized by $m \leq 30$, whereas the "fragile" ones have $m \geq 100$. If m falls within the range, $30 < m < 100$, the liquid is classified as intermediate glassformers.

The concept of fragility is currently of interest in the research fields such as formulation of amorphous drug and food preservation because it is considered as a key factor that correlates with the glass-forming ability and physical stability of the amorphous systems.[5,1,14−16] This is because the parameter m is related to an average degree of molecular mobility reflected in structural relaxation near the glass transition. "Fragile" glassformers have molecular mobility varies rapidly with temperature near T_g in contrast to that occurring in "strong" liquids. This difference has been considered by others to be the reason to expect that strong liquids are more physically stable than fragile liquids.

Fragility, manifests not only kinetically in the temperature dependence of log τ_α (i.e., different degrees of departures from the Arrhenius behavior) but also in thermal response of glassformers. Contrary to strong materials fragile liquids usually show large changes in thermal response (e.g., in the heat capacity C_p) near the glass transition. The fragile liquids are expected to have larger values of configurational heat capacities $C_{p,\mathrm{conf}}$, resulting from their configurational entropy changing rapidly with temperature, whereas the strong liquids have small $C_{p,\mathrm{conf}}$ because their configurational entropy only changes slowly with T.[13,17]

There are a lot of efforts to define a thermodynamic measure of fragility and predict the parameter m using calorimetric methods as well as to find a proper correlation between the dynamic fragility and thermodynamic fragility.[18−20]

Angell[13] proposed that thermodynamic measure of fragility can be a ratio of the heat capacities in the liquid and crystalline states C_p^l/C_p^cevaluated at T_g. In the case of materials that do not exhibit any crystalline form (as it is for many polymers) the ratio C_p^l/C_p^c is replaced with the ratio C_p^l/C_p^g in the liquid and glassy states.[18,21] Huang and McKenna[18] compared the dynamic and thermodynamic fragilities of many compounds from different classes of materials and showed that positive correlation between them (which was a commonly accepted picture) is not generally true. They obtained: (i) a increase in m with increasing C_p^l/C_p^c for inorganic glass formers; (ii) a decrease in m with increasing C_p^l/C_p^g for polymers; and (iii) a very weak correlation between m and C_p^l/C_p^c for small molecule organics and H-bonding small molecules.

Another thermodynamic parameter γ_{C_p}, which is often used to characterize fragility of pharmaceutical glass formers, is defined as follows[3,1,14,5]

$$\gamma_{C_p} = \frac{C_p^l - C_p^g}{C_p^l - C_p^c}^{T=T_g} = \frac{\Delta C_P}{C_{P,\mathrm{conf}}}^{T=T_g} \tag{4}$$

The value of γ_{C_p} can vary between 0 (for extremely fragile systems) and 1 (for extremely strong materials). The parameter γ_{C_p} is not only one of thermodynamic measures of fragility but it can be also exploited in the prediction of the temperature dependence of structural relaxation times in glass on the basis of Adam−Gibbs model,[22]

$$\tau_\alpha(T, T_f) = \tau_0 \exp\left(\frac{DT_0}{T(1 - T_0/T_f)}\right) \tag{5}$$

where T_f is the fictive temperature that can be estimated by using the following equation,

$$\frac{1}{T_f} = \frac{\gamma_{C_p}}{T_g} + \frac{1 - \gamma_{C_p}}{T} \tag{6}$$

Such a prediction enables us to evaluate a time scale of molecular motions reflected in the structural relaxation in the glassy state.

An empirical relation between dynamic and thermodynamic fragility has been proposed by Wang and Angell.[20,23,19] Taking into account experimental data for 42 materials they established the correlation

$$m = 56\frac{T_g \Delta C_P}{\Delta H_m} \tag{7}$$

which involves the jump in the heat capacity ΔC_P at T_g and the enthalpy of fusion ΔH_m.

On the basis of the random first-order transition theory, Lubchenko and Wolynes[24] derived a similar correlation,

$$m = 34.7\frac{T_m \Delta C_P}{\Delta H_m} \tag{8}$$

where T_m is the temperature of melting. The correlation was successfully tested for 44 substances belonging to different material classes.[19]

However, due to the complex nature of the glass transition these correlations are not ideally satisfied, and there are exceptions from these predictions. Therefore, further studies and experiments are necessary to verify the correlations between dynamic and thermodynamic fragility as well as to establish the most general one.

According to the correlation empirically established by Böhmer et al.,[8]

$$m_{p,\mathrm{corr}} = 250 \pm 30 - 320\beta_{\mathrm{KWW}} \tag{9}$$

fragile materials with large values of m should be characterized by broad structural relaxation peaks near T_g, that is, by high level of nonexponentiality of dielectric relaxation response (eq 1) or small value of β_{KWW}. On the other hand, strong glassformers (small m) should exhibit narrow relaxation peaks or large values of β_{KWW} in the vicinity of T_g. Faster modes of molecular motions within the spectrum of relaxation times can be responsible for nucleation in the glassy state; therefore, the more fragile glass former (of smaller β_{KWW}) would be more susceptible to nucleation.[25] Thus, β_{KWW} can be considered as the alternative parameter to the fragility index m for the purpose of correlating or predicting the physical stability of amorphous pharmaceutics. However, it should be noted that there are a few materials[26] that do not satisfied the correlation suggested by Böhmer et al.

There are many who believe that nucleation in the glassy state (where the α-relaxation times are too slow to be experi-

mentally observed) may also results from local molecular motions reflected in experiment as secondary relaxations.[25,2,27] In the glassy state, these faster secondary processes, called β, γ, etc., appear in the dielectric spectra. Therefore, in fact, these relaxations (having either inter- or intramolecular origin) provide us information on the molecular dynamics in the glassy state. Among different secondary relaxations, those reflecting motions of the whole molecule (intermolecular secondary relaxation) are of particular interest. The intermolecular local relaxation, also called Johari−Goldstein (JG) relaxation, is regarded as precursor of the molecular mobility of the cooperative α-relaxation. Studies of organic molecular glasses have shown that these localized motions, and not the long-range diffusion of α-relaxation process, determine the nucleation and crystallization rates in the glassy state.[25,27−30] The study of the JG relaxation is of fundamental importance because this process occurs in almost all the glass-forming systems, and the investigation of its relation with structural relaxation should allow deeper understanding of the glass transition phenomenon and provide an answer to the question of how the secondary processes influences crystallization of amorphous drugs.

In this paper we present results of dielectric relaxation study of the anti-inflammatory drug, celecoxib, in the liquid and glassy states. We show that dielectric spectroscopy can be applied very satisfactorily to monitor of molecular mobility of the material through measurements of its structural and secondary relaxation processes in the wide range of frequency and temperature. First we discuss the results for supercooled liquid celecoxib at temperatures above T_g. From the dielectric data we determine the fragility index m and the nonexponentiality parameter β_{KWW}, in order to check whether the Böhmer correlation is met in the case of celecoxib or not. Moreover, we test relations between kinetic and thermodynamic fragilities for the drug and check if the correlation between fragility and physical stability of amorphous celecoxib exists. Next, we analyze results obtained for the glassy state, especially the origin of the secondary relaxations. Finally, we attempt to draw a quantitative correlation between crystallization rate and the time scale of molecular mobility in the glassy state of celecoxib to determine what kind of molecular motions can be responsible for devitrification of celecoxib.

Experimental Methods

Material. The crystalline form of celecoxib of 98% purity and molecular mass of $M_w = 381$ g/mol was supplied from Polpharma (Starogard Gdanski, Poland). Celecoxib, 4-[5-(4-methylphenyl)-3-(trifluoromethyl)-1*H*-pyrazol-1-yl] benzenesulphonamide, belongs to a novel class of agents that selectively inhibit cyclooxygenase-2 (COX-2) enzymes. This is nonsteroidal anti-inflammatory drug used in the treatment of osteoarthritis, rheumatoid arthritis, and management of pain.[31] The chemical structures of the examined API is presented in Figure 1.

Broadband Dielectric Spectroscopy (BDS). Isobaric measurements of the dielectric permittivity $\varepsilon^*(\omega) = \varepsilon'(\omega) - i\varepsilon''(\omega)$ were carried out using the Novo-Control Alpha dielectric spectrometer over frequency range from 3×10^{-3} to 3×10^6 Hz at ambient pressure. Dielectric measurements of celecoxib were performed after its vitrification by fast cooling of the melt of crystalline form of celecoxib in a parallel-plate cell (diameter: 20 mm, gap: 0.1 mm). The sample temperatures in the range (153−371 K) were controlled by Quatro System using a nitrogen gas cryostat. The temperature stability was better than 0.1 K.

Differential Scanning Calorimetry (DSC). The standard differential scanning calorimetry measurements of celecoxib were carried out using Perkin-Elmer Pyris 1 DSC instrument with liquid nitrogen cooling. The crystalline and amorphous (prepared by quench-cooling of the melt of crystalline form in the open aluminum pan) samples were analyzed under helium purge (20 mL/min) in the hermetically sealed aluminum pans. The instrument was calibrated for temperature and heat flow using high-purity standards of indium and water. The thermal analysis was carried out between 313 and 453 K at a heating rate of 10 K/min.

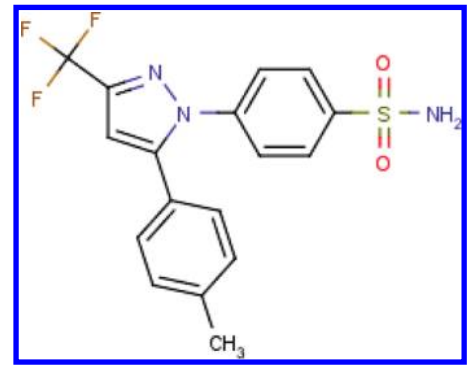

Figure 1. Chemical structure of celecoxib (CEL).

X-ray Diffraction. The X-ray diffraction (XRD) measurements were carried out at room temperature ($T = 293$ K) on the laboratory Rigaku-Denki D/MAX RAPID II-R difractometer attached with a rotating anode Ag Kα tube ($\lambda = 0.5608$ Å), an incident beam (0 0 2) graphite monochromator, and an image plate in the Debye−Scherrer geometry. The pixel size was 100 μm × 100 μm. Crystalline and amorphous samples of celecoxib were placed inside glass capillaries (1.5 mm in diameter). Measurements were performed for the sample-filled and empty capillaries, and the intensity for the empty capillary was then subtracted. The beam width at the sample was 0.1 mm. The two-dimensional diffraction patterns were converted into the one-dimensional intensity data using suitable software.

Results and Discussion

Nonisothermal and Isothermal Crystallization. Our study show that the amorphous celecoxib, prepared by quench-cooling of the melt of crystalline form, is highly unstable and recrystallizes at temperatures below its glass transition temperature T_g (during storage of the glass in isothermal conditions) as well as on heating the drug above T_g in the supercooled liquid temperature range.

The nonisothermal crystallization of the supercooled celecoxib (above its T_g) has been detected by means of DSC and dielectric measurements. Figure 2 presents DSC thermograms performed on heating (10 K/min) for crystalline and amorphous celecoxib. DSC-scan of stable crystalline form of celecoxib (Figure 2a) exhibits only melting endotherm in the temperature range of 436−441 K, whereas amorphous celecoxib (Figure 2b) prepared by quench-cooling shows several thermal effects: the glass transition at $T_g = 326$ K (determined as a midpoint of the glass transition step), cold crystallization exotherm in the temperature range of 365−376 K, and the melting endotherm in the temperature range of 429−444 K. It is worth noting that the non-isothermal cold crystallization phenomenon occurring on heating of amorphous celecoxib above its T_g has been also confirmed by dielectric measurements, and it will be presented later on in the paper in the subject concerning molecular mobility.

The isothermal crystallization studies of amorphous form of celecoxib (at room temperature $T = 293$ K, which corresponds

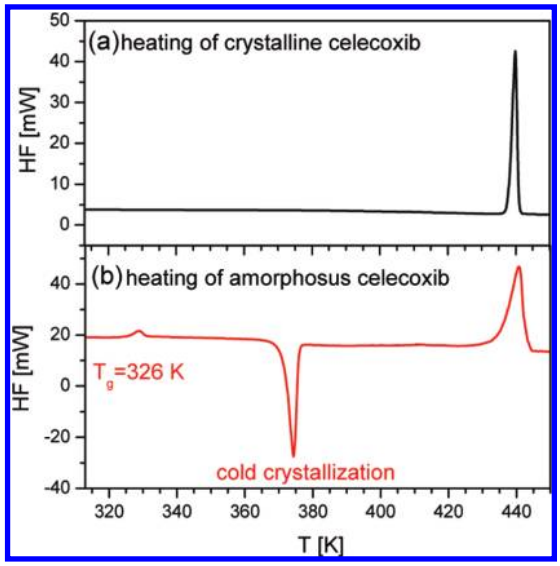

Figure 2. DSC thermograms for celecoxib performed on heating of the (a) crystalline and (b) amorphous forms.

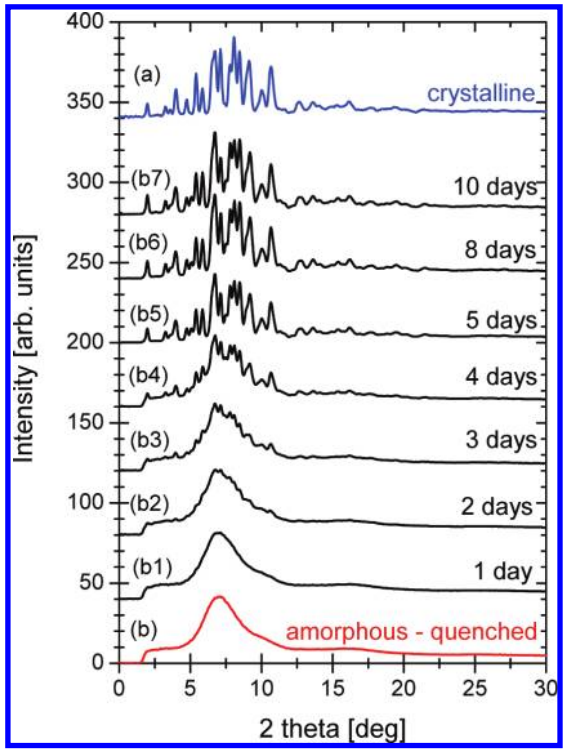

Figure 3. X-ray diffraction patterns for various solid-state forms of celecoxib performed at room temperature $T = 293$ K (33 K below its T_g): (a) the initial crystalline form of celecoxib; (b) amorphous celecoxib prepared by quench-cooling of the melt of crystal (a); (b1−b7) gradual isothermal recrystallization of the amorphous form (b) observed at specified time periods from 1 to 10 days.

to $T_g - 33$ K) have been performed by means of XRD, which is a very sensitive and foolproof method for solid-state characterization. Diffraction patterns for the initial crystalline form of celecoxib and its amorphous counterpart are presented in Figure 3, panels a and b, respectively. Very broad amorphous halos observed in Figure 3b in comparison with sharp Bragg peaks typical for crystalline state (see Figure 3a), confirm the lack of three-dimensional long-range ordered structure. This result indicates that the investigated sample was indeed prepared in the amorphous form. The capillary filled with the glassy celecoxib was stored at $T = 293$ K with quasi-constant humidity

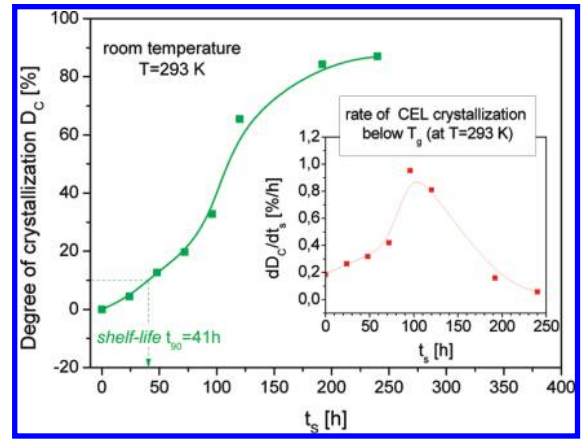

Figure 4. The relative degree of isothermal recrystallization D_C of amorphous celecoxib as a function of storage time t_S at $T = 293$ K. The inset presents the rate of celecoxib recrystallization evaluated as a derivative of D_c in terms of t_S. Solid lines are guides for eyes.

condition 10%. At specified time periods (i.e., after 1, 2, 3, 4, 5, 8, and 10 days) X-ray diffraction measurements were made, and the data can be seen in Figures 3b1−b7.

It is clearly seen that the area of sharp peaks increases with time, indicating that the degree of crystallization of the initial fully amorphous celecoxib increases. The intensity of the sharp XRD peaks observed in the case of the partly crystalline samples presented in Figures 3b1−b7 is constituted of both the crystalline and amorphous forms of celecoxib. We can evaluate the relative degree of crystallization D_c for each diffraction pattern as a ratio of areas of XRD peaks for a partly crystalline sample A_t and for the 100% crystalline sample A_0. The values $D_c = A_t/A_0$ are plotted as a function of storage time t_S (time that passed from preparation of the amorphous form of the celecoxib) in Figure 4. By calculating the derivative of D_c with respect to t_S we estimated that the maximal rate of recrystallization is achieved at about 100 h of storage (see the inset to Figure 4).

Molecular Mobility−Relaxation Dynamics. In Figure 5(a,b) we present dielectric spectra obtained during heating of amorphous celecoxib at atmospheric pressure with temperature changing from 153 to 371 K. To show the relaxation processes more clearly we divided the entire data set into two parts.

Panel a of Figure 5 presents relaxations above T_g, where the α-process dominates and carries information about the changes in the structure of the investigated sample. Here liquid-glass transition is defined to occur when the frequency of maximum loss of the α-relaxation process $f_{max} = 1.6 \times 10^{-3}$ Hz, which corresponds to structural relaxation time $\tau_\alpha = (1/2)\pi f_{max} = 100$ s. By analyzing the structural relaxation we can also detect cold crystallization of celecoxib. As can be seen in Figure 5a, the α-process peaks move toward higher frequencies on heating up to $T = 365$ K, which indicates the increase in molecular mobility of the system. At $T > 365$ K, the dielectric strength of the α-process, $\Delta\varepsilon_\alpha$, (proportional to the total amount of relaxing units participating in the structural process) begins to rapidly decrease (see Figure 6). Such a sudden drop in $\Delta\varepsilon_\alpha(T)$ is caused by the onset of the sample recrystallization on heating and reflects the increasing degree of crystallinity. This result is in good agreement with DSC measurements presented before in Figure 2b.

Panel b of Figure 5 presents spectra collected below T_g, that is, in the glassy state of celecoxib. In this region we observed only secondary processes because the α-relaxation is too slow to be measured. In the case of celecoxib we can distinguish as many as three secondary relaxations: the slowest β-process, the

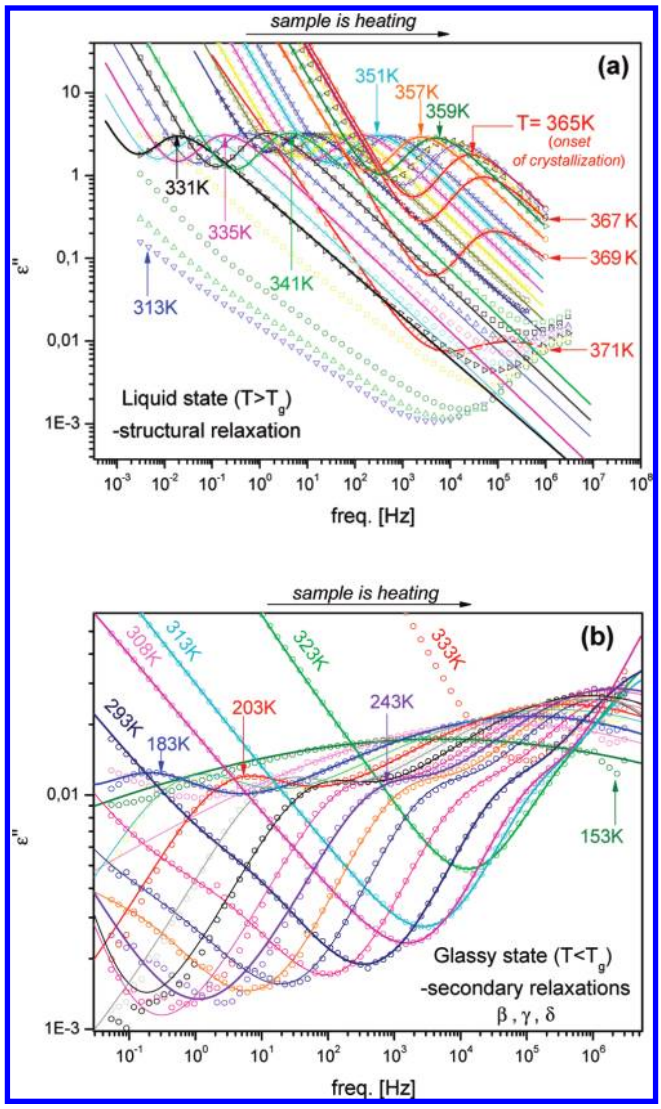

Figure 5. Dielectric loss spectra for celecoxib at different temperatures (a) above and (b) below T_g. Solids lines represent the spectra fits to eq 10.

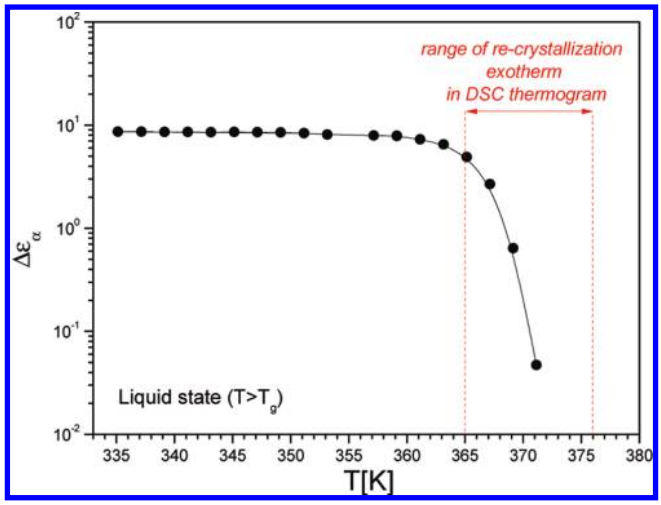

Figure 6. Temperature dependence of dielectric strength $\Delta\varepsilon_\alpha$ of α-relaxation for supercooled celecoxib.

faster γ-process, and the fastest δ-process (see Figure 7b). This finding proves high local molecular mobility in the glassy state of the drug. As can be seen in Figure 5b, secondary relaxations also moves toward lower frequencies with decreasing temperature, but they are far less sensitive to temperature changes than the α-relaxation. The nature of this relaxation will be discussed in a later part of this paper.

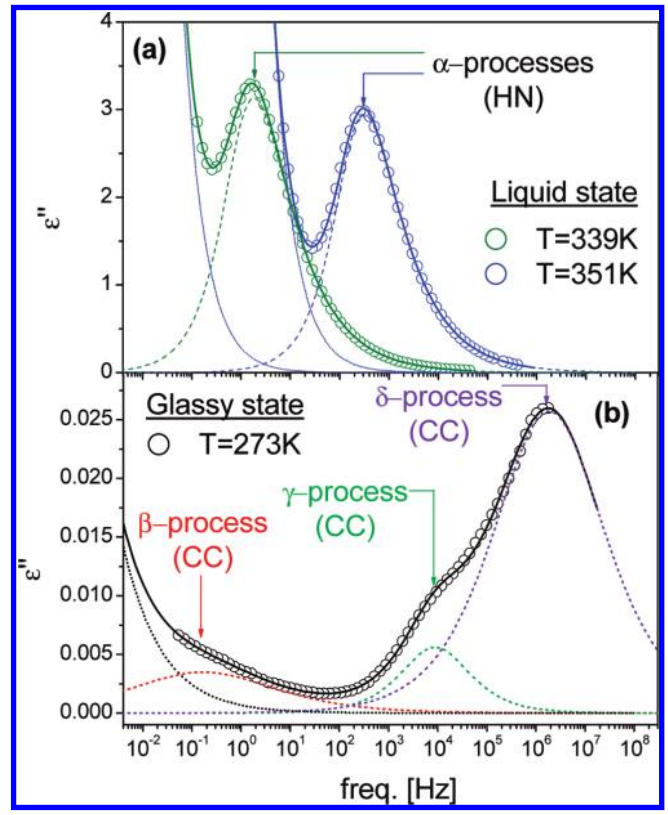

Figure 7. The examples of fitting procedure of selected dielectric loss spectra obtained in the (a) liquid and (b) glassy states of celecoxib. Solid lines depict fits of entire spectra based on the superposition of ionic conductivity and Havriliak−Negami (above T_g) and the superposition of three Cole−Cole functions (below T_g).

To precisely determine relaxation times of all the relaxation processes we carried out a numerical fitting analysis of the entire dielectric spectra as superposition of the Havriliak−Negami (HN) function describing the broad and asymmetric α peak and the Cole−Cole (CC) functions that well describe symmetric secondary relaxations. The complex permittivity $\varepsilon^*(\omega)$ data of quenched celecoxib are fitted to the following formula,

$$\varepsilon^*(\omega) = \varepsilon'(\omega) - i\varepsilon''(\omega) = \varepsilon_\infty + \sum_k \frac{\Delta\varepsilon_k}{[1 + (i\omega\tau_k)^{\xi_k}]^{\delta_k}} \quad (10)$$

Here, ε_∞ is the high frequency limit permittivity and k stands for either the primary and the secondary processes. $\Delta\varepsilon_k$ is the relaxation strength, τ_k is the HN relaxation time, and ξ_k and δ_k are the HN exponents of the relaxation processes. For secondary relaxation processes, δ_k is fixed to be equal to unity, so that the HN function becomes the CC function. Examples of the fitting procedure of dielectric spectra obtained in the liquid and glassy states are shown in Figure 7, panels a and b, respectively. Above T_g, spectra have been satisfactory fitted by a superposition of ionic conductivity and one HN function, whereas to describe dielectric spectra in the glassy state a superposition of three CC functions has been applied.

From the best fits of dielectric spectra we obtained the temperature dependences of the relaxation times of all dielectric processes for celecoxib (see Figure 8).

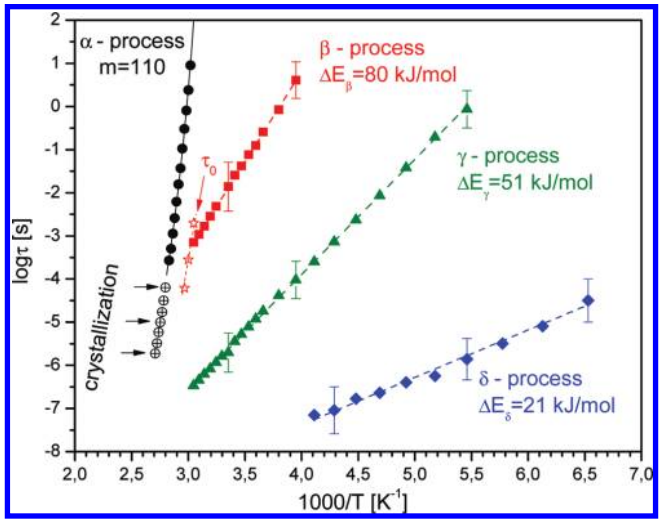

Figure 8. The relaxations map of celecoxib. Temperature dependence of structural relaxation times (solid circles) was fitted to VFT equation (solid line). Crossed circles show α-relaxation times above T_g in the crystallization range. Temperature dependences of secondary relaxations: β, γ, and δ were fitted to the Arrhenius equation (dotted lines). Open stars are the primitive relaxation times of the coupling model calculated with $\beta_{KWW} = 0.67$ at temperatures $T \approx T_g$.

TABLE 1: Comparison of the VFT Parameters Predicted from Thermal Methods by Gupta et al.[1] As Well As by Kaushal and Bansal[14] in Comparison with the Ones Obtained by Us from Dielectric Experiment (BDS)

material	log τ_∞	T_0 (K)	D	fragility m (for $\tau_\alpha = 100$ s)
celecoxib (BDS)	−14	280.2 ± 0.6	6.275 ± 0.075	110 ± 3
celecoxib (by Gupta et al.)	−14	246	11.5	67
celecoxib (by Kaushal and Bansal)	−14	267.7	8.8	83.3

Structural Relaxation Times and Fragility. The temperature dependence of the structural relaxation times $\tau_\alpha(T)$ can be described by the VFT equation (eq 2) with parameters collected in Table 1. It should be noticed that only α-relaxation times for the relaxation with nearly constant $\Delta\varepsilon_\alpha(T)$ have been fitted in order to avoid a possible influence of the partial crystallization on the values obtained for τ_α. The glass transition temperature $T_g = 328$ K has been evaluated by extrapolation of the VFT fit to $\log(\tau_\alpha/s) = 2$, which is in a good agreement with the value of $T_{g(DSC)} = 326$ K obtained from DSC measurement. On the basis of the VFT fit parameters, one can also calculate the dynamic fragility m according to eq 3. In this way we have established that celecoxib is characterized by a large value of isobaric fragility $m = 110$, which classifies the drug as a fragile material. It indicates that celecoxib exhibits a considerable molecular mobility near T_g, which correlates with its large tendency for crystallization. The correspondence between the large fragility and the ease of crystallization can be better realized within the framework of the two-order-parameter (TOP) model proposed by Tanaka.[32] According to this model, a liquid near the glass transition tends to order into the equilibrium crystal, but frustration effects of locally favored short-range ordering on long-range ordering prevent crystallization and help vitrification because the frustration effects increase the free-energy barrier for nucleation. It has been argued,[32] and later also supported by simulations,[33] that stronger frustration against crystallization makes a liquid stronger. In other words, the fragile system is easier to crystallize because its frustration against crystallization is weaker.

TABLE 2: Comparison of the Thermodynamic Parameters for Celecoxib by Gupta et al.[1] As Well As by Kaushal and Bansal[14]

thermodynamic parameters	Gupta et al.	Kaushal and Bansal
T_g [K]	323	331.4
T_m [K]	435.3	435
ΔH_m [J/g]		98.6
ΔC_P [J/gK]	0.26	0.44
$C_{P,conf}$ [J/gK]	0.56	0.50
T_{KS} [K]	246	267.7

We would like to draw the readers' attention to the many attempts that have been already made to predict the dynamic fragility parameter m for various pharmaceutical systems. One of the most popular approaches for this task is to estimate the VFT parameters by using calorimetric measurements.[34,1,14] On the basis of assumptions that (i) the VFT divergence temperature T_0 is equal to the Kauzmann temperature T_K, (ii) the preexponential factor representing the time scale of vibrational motions $\tau_0 = 10^{-14}$ s, and (iii) the structural relaxation time $\tau_\alpha = 100$ s at T_g, one can calculate the strength parameter D from the VFT equation (eq 2). Then, the value of the parameter m is calculated from eq 3. The key problem of this method is the evaluation of the proper value of T_K. There are many ways to approximate T_K. The simplest and the roughest ones are $T_K \approx T_g - 50$ K or $T_K \approx T_g^2/T_m$. More precise methods are based on configurational quantities, for example, $T_K = T_m - (\Delta H_m/C_{P,conf})$. Among of them the method exploiting the extrapolation of configurational entropy S_{conf} to zero is treated as the most important one: $TKS^{-1} = T_m^{-1}(1 + \Delta H_m/A)$, where $A = C_{P,conf}T$ is a nearly constant function of T. We would like to emphasize that values of T_K found[14,1] for celecoxib varies in the range almost of 50 K, depending on the method used to estimate T_K. It obviously leads to significant variations in the predicted values of the parameter m. Studying fragility of celecoxib, Gupta et al.[1] as well as Kaushal and Bansal[14] applied the favorably accepted method based on S_{conf} to evaluate the Kauzmann temperature T_{KS}. Using the same experimental technique of modulated temperature DSC (MTDSC) to measure the isobaric heat capacity of crystalline and amorphous celecoxib, the authors obtained considerably different results for thermal parameters (see Table 2). Consequently, they found correspondingly two different values of fragility index m (see Table 1). Both values are much smaller than the dynamic fragility m of celecoxib obtained from BDS technique directly from the measurements of molecular dynamics. It is worth noting that the values of fragility obtained by Gupta et al.[1] as well as Kaushal and Bansal[14] classify celecoxib as not a fragile but as an intermediate liquid. Using the predicted VFT parameters from thermal methods we simulated curves of the temperature dependences of structural relaxation times, and then we compared them with the one obtained by us from dielectric experiments. As can be seen in Figure 9, the dependences log $\tau_\alpha(T)$, estimated from calorimetric data, distinctly deviate from that found from relaxational data.

On the basis of thermodynamical parameters obtained from calorimetric measurements by the authors of refs 1 and 14 (see Table 2), we have also calculated the thermodynamic fragilities proposed by Wang and Angell (eq 7) and by Lubchenko and Wolynes (eq 8). Obtained values of the fragilities are collected in Table 3. Using thermodynamic parameters for celecoxib found by Gupta et al., the relations given by eqs 7 and 8 yield relatively small values of the parameter m that would situate

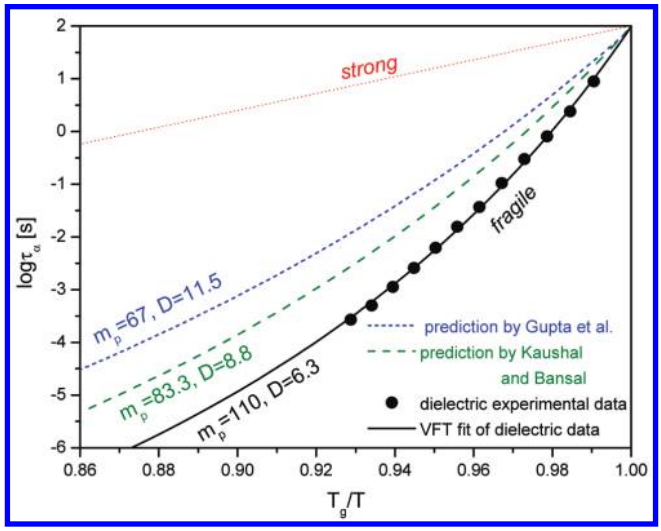

Figure 9. T_g-scaled temperature dependence of τ_α from the simulated curves of the temperature dependences of structural relaxation times performed on the basis of predicted VFT parameters from thermal methods by Gupta et al[1] (blue short dashed line) and Kaushal and Bansal[14] (green dashed line) in comparison with the one obtained by us directly from dielectric experiment (solid line).

TABLE 3: Predictions of the Fragility Parameter *m* in Terms of Eqs 7 and 8 for Celecoxib Evaluated on the Basis of Calorimetric Measurements Performed by Gupta et al.[1] As Well As by Kaushal and Bansal[14]

fragility parameter *m*	Gupta et al.	Kaushal and Bansal
m from eq 7	48	83
m from eq 8	40	67

the drug very close to strong materials (30 < intermediate fragility m < 100). On the other hand, the thermodynamic parameter established by Kaushal and Bansal leads to the considerably larger but still in the intermediate fragility range on the basis of eqs 7 and 8. Thus, there is also no correlation between such thermodynamically evaluated fragilities and the dynamic or kinetic fragility calculated from dielectric measurements in the case of celecoxib. Taking into account of the large tendency of celecoxib to crystallize, among various measures of fragility, only the dynamic fragility m having the largest value is capable to correlate with the physical instability of the amorphous drug.

It is worth noting that the authors[1,14] also analyzed another thermodynamic measure of fragility γ_{C_p} (eq 4) for celecoxib. Results of their analyses can create some confusion. According to the value of $\gamma_{C_p} = 0.46$ found by Gupta et al., celecoxib would be a more fragile material than it follows from the value of $\gamma_{C_p} = 0.875$ established by Kaushal and Bansal, because of the relation of the parameter γ_{C_p} to fragility given by: extremely fragile $0 < \gamma_{C_p} < 1$ extremely strong. It is in contradiction with their VFT-based predictions of the dynamic fragility m as well as with the values of m estimated from eqs 7 and 8. It suggests that there is no simple correlation between such measures of the fragility.

According to the correlation of Böhmer et al. (eq 9), fragile materials like celecoxib should be characterized by broad structural relaxation loss peaks in the vicinity of T_g, that is, smaller value of β_{KWW}. We can determine a value of the β_{KWW} parameter for the drug by fitting the α-loss peak in the frequency domain by means of the one-sided Fourier transform of the KWW function (eq 1), as shown in the right-hand-side of the following equation.

$$\varepsilon''_\alpha(\omega) = \Delta\varepsilon_\alpha \int_0^\infty \left[-\frac{d\Phi}{dt}\right] \sin(\omega t)\, dt \qquad (11)$$

The parameter $\Delta\varepsilon_\alpha$ denotes the dielectric strength of the α relaxation.

In Figure 10 we show that the shapes of structural relaxation peaks for celecoxib near T_g are almost independent of T (time−temperature superposition is valid for celecoxib). From the fit of the α-loss peaks by (eq 11), we found that the exponent β_{KWW} describing breadth of structural relaxation peak is equal to 0.67 (i.e., $n = 0.33$) near T_g. This small degree of nonexponentiality would suggest that celecoxib should be a relatively strong liquid and has a small tendency to crystallization.[25] Assuming that the Böhmer correlation: $m_{p,corr} = m_0 - s\beta_{KWW}$ (where $m_0 = 250$, $s = 320$) is applicable to celecoxib, it would predict $m_{p,corr} = 36 \pm 30$ for celecoxib. However, the real value of fragility determined from eq 3 is equal to $m = 110 \pm 3$. This is a large value of m that classifies celexoxib instead as a fragile glass formers. Thus, the behavior of celecoxib [similarly as propylene carbonate (PC) and cresolphthalein-dimethylether (KDE)] diverges from the expected correlation between parameters m and β_{KWW}. Therefore, one should be careful to use the correlation to predict the fragility parameter m (if one knows β_{KWW}) or the degree of dynamic heterogenity (if one knows m) because celecoxib is not the only exception to this correlation.

Glass Dynamics. Now we consider the molecular mobility in the glassy state of celecoxib that is reflected in secondary relaxation processes. As can seen in Figure 3, the temperature dependences of three secondary relaxation times (τ_β, τ_γ, and τ_δ) can be well-described by an Arrhenius equation,

$$\tau(T) = \tau_\infty \exp\left(\frac{\Delta E}{kT}\right) \qquad (12)$$

where τ_∞ is pre-exponential factor, ΔE is energy barrier and k is Boltzmann constant. As a result, we obtained the following fitting parameters: $\log \tau_{\infty\beta} = -15.87$, $\Delta E_\beta = 80$ kJ/mol for the slowest β-relaxation; $\log \tau_{\infty\gamma} = -14.59$, $\Delta E_\gamma = 51$ kJ/mol for γ-relaxation; and $\log \tau_{\infty\delta} = -11.78$, $\Delta E_\delta = 21$ kJ/mol for the fastest δ-process.

Various secondary relaxations that occur in the glassy state can have different molecular origin. The intermolecular secondary relaxation or the Johari−Goldstein (JG) process originates from motions of entire molecules or essentially all parts of the molecule in the case of nonrigid molecules. The intramolecular secondary relaxation or non-JG process comes from motion involving only a subset of the entire molecule. From this distinction, naturally the slowest secondary relaxations is usually the JG β-relaxation. For physical stability of amorphous drugs, the genuine JG secondary relaxation is the most interesting because it is often regarded as a trigger of recrystallization of the glass.[27−30,35] Therefore, the identification of which of the different secondary relaxations is a true JG-relaxation and recognition of its dynamical properties seems to be necessary in predicting the stability of the amorphous pharmaceutical.

Using the criteria of Ngai and Paluch[36] based on the extended Coupling Model (CM),[37] we can distinguish the intermolecular from intermolecular character of the three secondary relaxations exhibited by celecoxib.

The genuine JG relaxation is the precursor of structural relaxation (a local molecular motions which leads to the

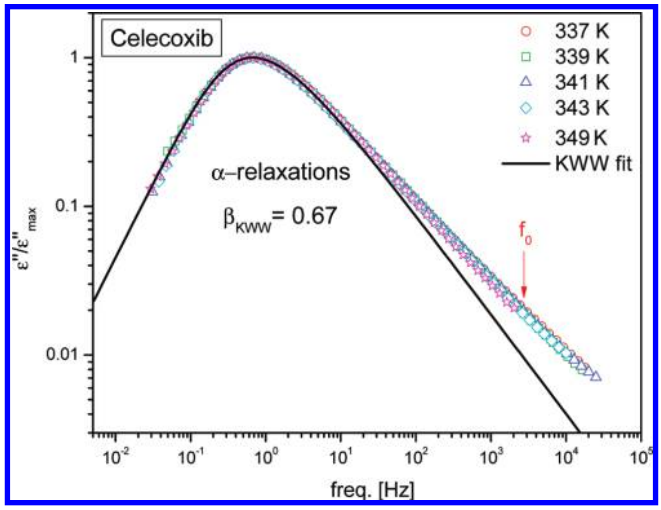

Figure 10. Time−temperature superposition for celecoxib: the α-loss peaks measured at various temperatures near T_g were shifted horizontally to the maximum of reference spectra obtained at $T = 337$ K (α-relaxation peaks are practically independent of T). The solid line represents the fit of the α-process peaks by the KWW function (eq 11). The vertical arrow indicates f_0 at $T = 337$ K, which corresponds to $(1/2\pi\tau_0)$, where τ_0 is the primitive relaxation time calculated from eq 14.

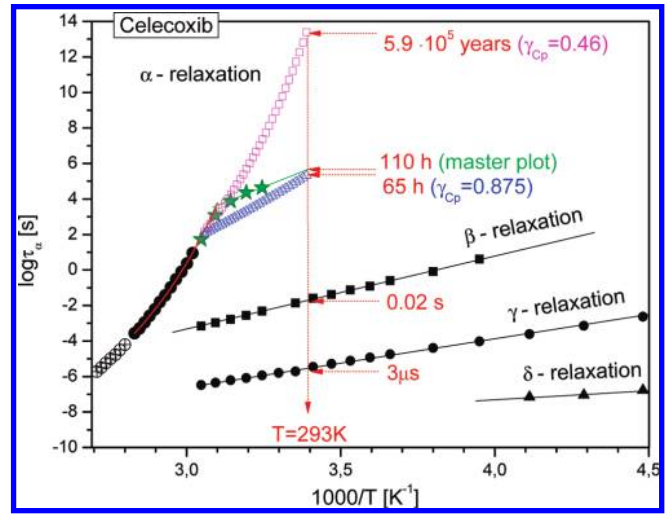

Figure 11. Prediction of structural relaxation times in the glassy state and time scales of molecular motions at the temperature of storage of amorphous celecoxib $T = 293$ K. Open magenta squares and open blue triangles denote predicted $\tau_\alpha(T < Tg)$ from extended AG model with $\gamma_{C_p} = 0.46$[1] and $\gamma_{C_p} = 0.875$,[14] respectively. Solid green stars indicate $\tau_\alpha(T < T_g)$ predicted on the basis of the master plot.

α-relaxation), therefore its relaxation time τ_{JG} should correspond well to the primitive relaxation time τ_0 of the CM, that is,

$$\tau_{JG} \approx \tau_0 \tag{13}$$

The CM relates the primitive relaxation time τ_0 to the structural relaxation time τ_α, at any temperature T and pressure P, by the following equation,

$$\tau_0 = (t_c)^n(\tau_\alpha)^{1-n} \tag{14}$$

where $n = 1 - \beta_{KWW}$ from the KWW function (eq 1) used to fit the α-loss peak, and t_c is equal to 2 ps for small molecular and polymeric glass formers.

For celecoxib, the values of primitive relaxation time τ_0 at several temperatures above T_g from 337 to 328 K have been calculated by eq 14 using the previously determined parameter $\beta_{KWW} = 0.67$ and structural relaxation times τ_α from the VFT fit (solid line in Figure 8). Also the calculated primitive relaxation frequency ($f_0 = 1/2\pi\tau_0$) of the CM for the spectra measured at $T = 337$ K is shown in Figure 10 as an example. It can be seen that the value determined for f_0 lies within the range of frequencies where the KWW fit deviates from experimental data and the excess wing is observed. It indicates that there exists a secondary relaxation coming from intermolecular motions, which is hidden under the dominant α-peak. One can see that the locations of the calculated τ_0 indicated by the open stars in Figure 8 are consistent with β-relaxation times τ_β found at T close to T_g (i.e., $\tau_0 \approx \tau_\beta$). Change from the Arrhenius T-dependence to stronger temperature dependence of τ_β after crossing T_g from below is suggested by the calculated τ_0 above T_g as shown in Figure 8. The spectra of celecoxib taken above T_g do not allow us to resolve the β-relaxation and determine τ_β, and hence comparison with the calculated τ_0 cannot be made to verify the change in T-dependence. However, there are many other glassformers in which this change in T-dependence of τ_β has been seen.[38] Thus, one may classify the β-relaxation of the quenched celecoxib as the primitive or the JG β-process that has an intermolecular character and can play a potential role in devitrification of the drug. The opinion that β-relaxation reflects a local motion of the entire molecule is supported by the high value of activation energy of the β-process ($\Delta E_\beta = 80$ kJ/mol) (see Figure 8). Another conclusion that can be drawn from this consideration is that the faster secondary relaxations (γ and δ) characterized by smaller values of activation energies ($\Delta E_\gamma = 51$ kJ/mol and $\Delta E_\delta = 21$ kJ/mol) originate from intramolecular motions of smaller parts of the celecoxib molecules, therefore their influence on physical stability of amorphous celecoxib seems to be not significant.

As a final point we compare time scales of molecular motions reflected in structural and secondary relaxations in the glassy state of celecoxib to make an attempt to assess which kind of molecular motion is most responsible for recrystallization of the amorphous drug at storage temperature ($T = 293$ K). In this context, a key problem is to reliably predict structural relaxation times in glass that are too long to be experimentally found. The models commonly used to describe the temperature dependences of α-relaxation times (i.e., the VFT equation) in the supercooled liquid region do not explain deviations from equilibrium behavior, and consequently they cannot be used to properly estimate τ_α(T) below T_g. However, the Adam and Gibbs' (AG) model[22] has been extended into the glassy state (eqs 5 and 6).[3,17,5]

We apply this extended AG model to predict the dependence $\tau_\alpha(T)$ for celecoxib at $T < T_g$. We assume that the parameters τ_∞, D, and T_0 in eq 5 collected in Table 1 can be taken from fitting the temperature dependence of α-relaxation times above T_g by means of the VFT equation (eq 2), whereas the fictive temperature T_f for each $T < T_g$ are calculated according to eq 6 by using the thermodynamic parameter $\gamma_{C_p} = 0.46$ found by Gupta et al.[1] as well as $\gamma_{C_p} = 0.875$ established by Kaushal and Bansal.[14] As can be seen in Figure 11 we obtain completely divergent results of the prediction. It is a consequence of the big difference between the used values of γ_{C_p} that yield a nearly Arrhenius behavior for the larger value reported by Kaushal and Bansal and a distinctly non-Arrhenius dependence for the smaller one obtained by Gupta et al.

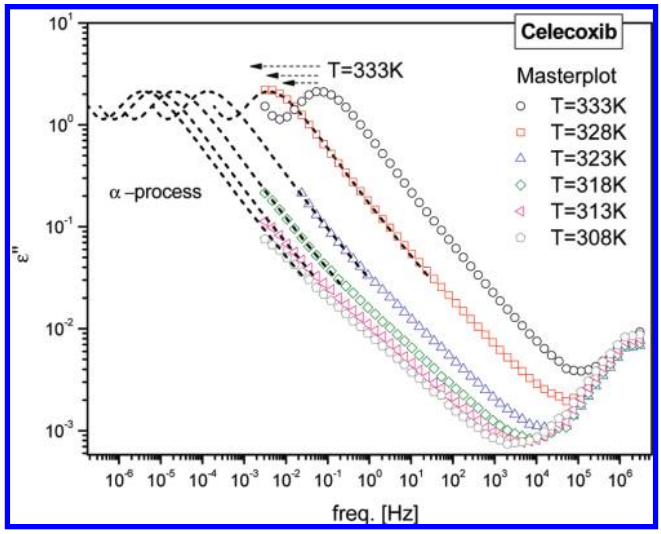

Figure 12. Masterplot for celecoxib constructed by horizontally shifting the loss peak at 333 K to overlap loss spectra at 328, 323, 318, 313, and 308 K.

Since the thermodynamically evaluated parameter γ_{C_p} introduces a large uncertainty about the prediction of $\tau_\alpha(T)$ by means of eq 5, we use also another method for estimation of the structural relaxation times at $T < T_g$ that is based only on dynamic measurements (BDS). This approach consists in construction of a master plot by horizontally shifting the α-loss peak very well visible in the liquid state but near T_g to lower frequencies in order to overlap loss spectra collected at lower temperatures ($T < T_g$) for which it was measured only high frequency flanks of the α-loss peak. Such an evaluation of the α-peak positions below T_g is permitted only if the shape of structural relaxation peak is almost temperature independent and the time−temperature superposition (TTS) occurs. It is shown in Figure 10 that the TTS is valid for $T \geq T_g$ in the case of celecoxib, therefore we can expect that it remains justified in some limited temperature range below T_g. Thus, we can construct the master plot for celecoxib with the reference spectrum at 333 K to predict positions of the α-peak maxima at several temperatures below T_g (see Figure 12). As a result we obtain α-relaxation times (stars in Figure 11) in the glassy state that are in fair agreement with those predicted from eqs 5 and 6 by using γ_{C_p} reported by Kaushal and Bansal. Taking into account the achieved agreement between the results obtained from two different methods one can claim that the structural relaxation times predicted from the master plot and from the extended AG model with $\gamma_{C_p} = 0.875$ are definitely more reliable than those found from the extended AG model with $\gamma_{C_p} = 0.46$. Thus, if we consider the temperature of storing amorphous celecoxib to be $T = 293$ K, which is over 30 K below T_g, we can evaluate the time scale of molecular motions in the structural relaxation can be within the range of 65−110 h than the extremely high values $\sim 10^5$ years predicted by using the extended AG model with $\gamma_{C_p} = 0.46$. It is worth noting that the maximum rate of recrystallization of amorphous celecoxib at 293 K occurs in the range of 80−120 h (see Figure 4), which corresponds to the predicted time scale of α-relaxation at the same temperature. Moreover, the shelf life t_{90} of amorphous celecoxib (defined as the time interval after which 90% of the drug remains still amorphous, often regarded as a measure of crystallization rate) is equal 41 h at 293 K (see Figure 4). It is also very close to the predicted structural relaxation time at this temperature. Therefore, the structural relaxation seems to be responsible for devitrification of celecoxib at $T = 293$ K. However, the role of the secondary JG relaxation (characterized by much faster molecular motions, i.e., $\tau_\beta = 0.02$s at 293 K) in crystallization cannot be under appreciated, because the intermolecular secondary JG β-process acts as the precursor of the structural α-relaxation. The JG β-process being directly responsible for crystallization deep in the glassy state was proposed by Oguni and co-workers[27−30] based on evidence from their own experimental studies. There are different views of molecular mechanism for crystallization deep in the glassy state have been offered by others.[39−41] Konishi and Tanaka[39] considered the role of volume contraction ΔV on crystallization. They went on to proposed, for a material having large ΔV, the volume contraction upon crystallization provides a crystal-glass interface with large excess free volume, which results in the mobility increase at the growth front and leads to enhancement of the crystal growth. Taking into account that the translational diffusion is considered[42−45] to be effective for crystallization in the equilibrium liquid state, the authors[39,45] suggest an important role of this factor in the crystal growth also in the glassy state. Our study has no way to check the validity of these proposals. On the other hand, Xie et al.[40] and Sun et al.[41] concluded otherwise that their observed dependences of crystal growth of ortho-terphenyl (OTP) and 5-methyl-2-[(2-nitrophenyl)amino]-3-thiophenecarbonitrile (ROY) deep in the glassy state does not originate from the JG β-process. The deduction by Xie et al. for OTP was based on the JG β-relaxation observed by dielectric spectroscopy in glassy *o*-terphenyl disappearing with time[46] too quickly to be related to crystal growth, which continues to be observed in glassy OTP. This conclusion, that the existence of a secondary relaxation peak is not a necessary condition for observing crystallization deep in the glassy state, was reinforced by Sun et al. for ROY because they failed to find any evidence of the JG β-relaxation from dielectric measurements. This conclusion can be premature in view of the following facts about JG β-relaxation and its observation by dielectric spectroscopy. Usually the dielectric strength of the α-relaxation is much larger than that of the JG β-relaxation. OTP has a very small dipole moment. Its α-relaxation has small dielectric strength, hence the dielectric strength of its JG β-relaxation is even smaller and is barely detectable by rapid quenching into the glassy state. As the glass is densified by physical aging with time, the amplitude of the JG β-relaxation is reduced, resulting in decrease of its already small dielectric strength and hence becoming undetectable after some time. The "disappearance" of the JG β-dielectric loss peak in glassy *o*-terphenyl with time is a problem specific to dielectric spectroscopy and does not mean that the motion corresponding to the JG β-relaxation no longer exists. In fact, Fujimori and Oguni[47] found the JG β-relaxation of OTP, propylene carbonate, and other glassformers by adiabatic calorimetry at $\tau_\beta = 1$ ks at temperature $T_{g\beta}$ much lower than T_g, thus the presence of the JG β-relaxation is not in doubt. Accompanying the reduction of relaxation strength on physical aging is the shift of the relaxation time τ_β to larger values. The shift of τ_β to longer times is much less than that of τ_α as expected from eq 14, and this can explain the observed slowing down of the crystal growth rate by 30% with time, whereas other causes considered by Xie et al. and Sun et al. cannot. The JG β-relaxation of ROY cannot be resolved in the liquid, and a glassy state also cannot be used to conclude that it does not exist in ROY. ROY has a large KWW exponent, $\beta_{KWW} \equiv (1 - n) = 0.73$, comparable to that of glycerol, propylene glycol, and propylene carbonate.[48] From the well established correlation between the ratio $\log(\tau_\alpha/\tau_\beta)$ and n,[36,37] it is clear that τ_β is not much shorter than τ_α, hence it is not resolved and appear as the excess wing in the dielectric spectrum. This possibility was mentioned by Sun et al. It is worthwhile to reiterate that the JG β-relaxation of propylene carbonate not detected by dielectric spectroscopy was found by adiabatic calorimetry at $\tau_\beta = 1$ ks deep in the glassy state. The

discussion above is given for the purpose of removing the doubt cast on the JG β-relaxation for its role in crystallization deep in the glassy state.

Conclusions

It has been recognized by using BDS, DSC, and XRD that amorphous celecoxib prepared by quench-cooling of the melt of its crystalline form is physically unstable and is easy to recrystallize below and above T_g. By using dielectric spectroscopy we found the dynamic fragility index for celecoxib is $m = 110$, which allows us to classify this drug as a fragile liquid. The large value of m indicates a large average degree of molecular mobility of structural relaxation near the glass transition, and it correlates with the large tendency of celecoxib to crystallization. However, values of the fragility m evaluated on the basis of thermodynamic parameters turns out to have been significantly underestimated, suggesting that celecoxib has intermediate fragilities and do not account for the ease of celecoxib to crystallize. Therefore, in the case of celecoxib we established that only the dynamic fragility m is capable of predicting the physical stability of the amorphous drug. Moreover, there is no correlation between the thermodynamically evaluated fragilities and the dynamic fragility m calculated directly from dielectric structural relaxation times.

We found that celecoxib do not satisfy the correlation between the parameter m and the degree of dynamic heterogeneity ($1 - \beta_{KWW}$). The drug is characterized by a relatively narrow structural relaxation peak in comparison with the large value of m. Since it is considered that a narrow distribution of α-relaxation times is related to a small tendency of amorphous drug to crystallization, therefore the parameter β_{KWW} cannot be used to predict stability of celecoxib against crystallization.

Making a prediction of the α-relaxation times in the glassy state we estimated the time scale of molecular motion in the structural relaxation below T_g. We found that τ_α at the temperature of storage of amorphous celecoxib, $T = 293$ K, corresponds to the time of maximum rate of recrystallization of amorphous celecoxib at this temperature. It leads to the conclusion that just the structural relaxation seems to be mainly responsible for devitrification of celecoxib. Moreover, the recrystallization of amorphous celecoxib can be affected by the large molecular mobility reflected by the three secondary relaxations, among which the β-process can play an important role because we have verified that it is the true JG relaxation involving intermolecular motions of the entire molecule, and hence it is a precursor of the structural α-relaxation.

Acknowledgment. The authors are deeply thankful for the financial support of their research within the framework of the project entitled "From Study of Molecular Dynamics in Amorphous Medicines at Ambient and Elevated Pressure to Novel Applications in Pharmacy" (Contract No. TEAM/2008-1/6), which is operated within the Foundation for Polish Science Team Programme cofinanced by the EU European Regional Development Fund. Moreover, K.G. thanks FNP for awarding grants within the framework of the START Programme (2009).

References and Notes

(1) P. Gupta, P.; Chawla, G.; and; Bansal, A. K. *Mol. Pharm.* **2004**, *1* (6), 406–413.
(2) Bhugra, C.; Pikal, M. J. *J. Pharm. Sci.* **2008**, *97*, 1329–1349.
(3) Shamblin, S. L.; Tang, X.; Chang, L.; Hancock, B. C.; Pikal, M. J. *J. Phys. Chem. B* **1999**, *103*, 4113–4121.
(4) Shamblin, S. L.; Hancock, B. C.; Dupuis, Y.; Pikal, M. J. *J. Pharm. Sci.* **2000**, *89*, 417–427.
(5) Hancock, B. C.; Shamblin, S. L. *Thermochim. Acta* **2001**, *380*, 95–107.
(6) Williams, G.; Watts, D. C. *Trans. Faraday Soc.* **1970**, *66*, 80–85.
(7) Roland, C. M.; Hensel-Bielowka, S.; Paluch, M.; Casalini, R. *Rep. Prog. Phys.* **2005**, *68*, 1405–1478.
(8) Böhmer, R.; Ngai, K. L.; Angell, C. A.; Plazek, D. J. *J. Chem. Phys.* **1993**, *99*, 4201–4209.
(9) Vogel, H. *J. Phys. Z.* **1921**, *22*, 645–646.
(10) Fulcher, G. S. *J. Am. Ceram. Soc.* **1925**, *8*, 339–355.
(11) Tammann, G.; Hesse, W. *Z. Anorg. Allg. Chem.* **1926**, *156*, 245–257.
(12) Angell, C. A. *Polymer* **1997**, *38*, 6261–6266.
(13) Angell, C. A. *J. Non-Cryst. Solids* **1991**, *131−133*, 13–31.
(14) Kaushal, A. M.; Bansal, A. K. *Eur. J. Pharm. Biopharm.* **2008**, *69*, 1067–1076.
(15) Perera, D. N. *J. Phys.: Condens. Matter* **1999**, *11*, 3807–3812.
(16) Lu, Z. P.; Li, Y.; Liu, C. T. *J. Appl. Phys.* **2003**, *93*, 286–290.
(17) Hodge, I. M. *J. Non-Cryst. Solids* **1996**, *202*, 164–172.
(18) Huang, D.; McKenna, G. B. *J. Chem. Phys.* **2001**, *114*, 5621–5630.
(19) Stevenson, J. D.; Wolynes, P. G. *J. Phys. Chem. B* **2005**, *109*, 15093–15097.
(20) Wang, L.-M.; Velikov, V.; Angell, C. A. *J. Chem. Phys.* **2002**, *117*, 10184–10355.
(21) Simon, S. L.; Plazek, D. J.; Sobieski, J. W.; McGregor, E. T. *J. Polym. Sci., Part B: Polym. Phys.* **1997**, *35*, 929–936.
(22) Adam, G.; Gibbs, J. H. *J. Chem. Phys.* **1965**, *43*, 139–146.
(23) Wang, L.-M.; Angell, C. A. *J. Chem. Phys.* **2003**, *118*, 10353–10355.
(24) Lubchenko, V.; Wolynes, P. G. *J. Chem. Phys.* **2003**, *119*, 9088–9105.
(25) Tombari, E.; Ferrari, C.; Johari, G. P.; Shanker, R. M. *J. Phys. Chem. B.* **2008**, *112*, 10806–10814.
(26) Paluch, M.; Ngai, K. L.; Hensel-Bielowka, S. *J. Chem. Phys.* **2001**, *114*, 10872–10883.
(27) Hikima, T.; Hanaya, M.; Oguni, M. *J. Mol. Struct.* **1999**, *479*, 245–250.
(28) Hikima, T.; Hanaya, M.; Oguni, M. *Chem. Soc. Jpn.* **1996**, *69*, 1863–1868.
(29) Paladi, F.; Oguni, M. *Phys. Rev. B.* **2002**, *65*, 144202–144207.
(30) Paladi, F.; Oguni, M. *J. Phys.: Condens. Matter* **2003**, *15*, 3909–3917.
(31) Chawla, G.; Gupta, P.; Thilagavathi, R.; Chakraborti, A. K.; Bansal, A. K. *Eur. J. Pharm. Sci.* **2003**, *20*, 305–317.
(32) Tanaka, H. *J. Non-Cryst. Solids* **2005**, *351*, 678–690.
(33) Shintani, H.; Tanaka, H. *Nature Phys.* **2006**, *2*, 200–206.
(34) Crowley, K. J.; Zografi, G. *Thermochim. Acta* **2001**, *380*, 79–93.
(35) Oguni, M. *J. Non-Cryst. Solids* **1997**, *210*, 171–177.
(36) Ngai, K. L.; Paluch, M. *J. Chem. Phys.* **2004**, *120*, 857–873.
(37) Ngai, K. L. *J. Phys.: Condens. Matter* **2003**, *15*, S1107.
(38) Ngai, K. L.; Casalini, R.; Capaccioli, S.; Paluch, M.; Roland, C. M. Dispersion of the Structural Relaxation and the Vitrification of Liquids; 2006; Vol. 133, Part B, Ch. 10, pp 497−593.
(39) Konishi, T.; Tanaka, H. *Phys. Rev. B* **2007**, *76*, 220201.
(40) Xi, H.; Sun, Y.; Yu, L. *J. Chem. Phys.* **2009**, *130*, 094508.
(41) Sun, Y.; Xi, H.; Ediger, M. D.; Richert, R.; Yu, L. *J. Chem. Phys.* **2009**, *131*, 074506.
(42) Ngai, K. L.; Magill, J. H.; Plazek, D. J. *J. Chem. Phys.* **2000**, *112*, 1887–1892.
(43) Mapes, M. K.; Swallen, S. F.; Ediger, M. D. *J. Phys. Chem. B* **2006**, *110*, 507–511.
(44) Masuhr, A.; Waniuk, T. A.; Busch, R.; Johnson, W. L. *Phys. Rev. Lett.* **1999**, *82*, 2290–2293.
(45) Tanaka, H. *Phys. Rev. E* **2003**, *68*, 011505−1 - 011505−8.
(46) Wagner, H.; Richert, R. J. *Phys. Chem. B* **1999**, *103*, 4071–4077.
(47) Fujimori, H.; Oguni, M. *Solid State Commun.* **1995**, *94*, 157–162.
(48) Ngai, K. L.; Lunkenheimer, P.; Leon, C.; Schneider, U.; Brandt, R.; Loidl, A. *J. Phys. Chem.* **2001**, *115*, 1405.

JP1040212